IOP Conf. Series: Materials Science and Engineering **330** (2018) 012033 doi:10.1088/1757-899X/330/1/012033

Influence of Welding Process and Post Weld Heat Treatment on Microstructure and Pitting Corrosion Behavior of Dissimilar Aluminium Alloy Welds

Venkata Ramana V S N[1*], Raffi Mohammed[2], Madhusudhan Reddy G[3] Srinivasa Rao K[4]

[1] Department of Mechanical Engineering, GITAM University, Visakhapatnam, India
[2]Department of Metallurgical& Materials Engineering, NIT-Andhra Pradesh, India
[3]Metal Joining Group, Defence Metallurgical Research Laboratory, Hyderabad, India
[4]Department of Metallurgical Engineering, Andhra University, Visakhapatnam, India

*Corresponding author E-mail: vsnvr@yahoo.com

Abstract. Welding of dissimilar Aluminum alloy welds is becoming important in aerospace, shipbuilding and defence applications. In the present work, an attempt has been made to weld dissimilar aluminium alloys using conventional gas tungsten arc welding (GTAW) and friction stir welding (FSW) processes. An attempt was also made to study the effect of post weld heat treatment (T4 condition) on microstructure and pitting corrosion behaviour of these welds. Results of the present investigation established the differences in microstructures of the base metals in T4 condition and in annealed conditions. It is evident that the thickness of the PMZ is relatively more on AA2014 side than that of AA6061 side. In FS welds, lamellar like shear bands are well noticed on the top of the stir zone. The concentration profile of dissimilar friction stir weld in T4 condition revealed that no diffusion has taken place at the interface. Poor Hardness is observed in all regions of FS welds compared to that of GTA welds. Pitting corrosion resistance of the dissimilar FS welds in all regions was improved by post weld heat treatment.

1. Introduction

Many emerging applications in industries like chemical, power generation, petrochemical, nuclear, aerospace, transportation and electronics lead to the joining of dissimilar materials by various joining techniques. Combinations of different metals in components provide a great flexibility in design and production and an optimized use of material properties. Welding of dissimilar aluminium alloys has gained importance in industry as it suits the light weight structures of complex design at minimum cost and having minimum weight [1]. The major problems in welding dissimilar metals are variation in melting point, thermal conductivity and coefficient of thermal expansion. The differences in thermal conductivity result in different heat input requirements for the individual alloys. Heat produced by the arc will flow more rapidly in the material having higher thermal conductivity which results in excess melting or burn through in the alloy having low thermal conductivity [2]. Furthermore, the filler metal requirements (dependent on the chemical composition of the base alloy) can be significantly different for the individual base alloys. Most of the age-hardenable aluminum alloys when welded with fusion welding processes either to themselves or with different alloys exhibit problems such as solidification cracking, porosity and inter-dendritic or intergranular segregation of solute elements leading to poor corrosion resistance and mechanical properties. When aluminium is alloyed with elements like copper, magnesium and silicon, they contribute in strengthening of these alloys by age hardening. In view of the limited solubility of these elements in aluminium, they are not only distributed in the aluminum solid solution but also are distributed as fine precipitates and coarse intermetallic particles. The

particles like $CuAl_2$ and Mg_2Si in general will have a great role to play in the welding of aluminum alloys especially heat treatable aluminium alloys which generally induce liquation in the partially melted zone (PMZ). The heat treatable aluminum alloys are susceptible to crack in the partially melted zone (PMZ) of the weld. The studies by Huang and Kou include the mechanisms of liquation and they found that significant weakening of PMZ is caused by grain boundary segregation [3-6]. Though it is preferred to use alternating current GTA welding process for aluminum alloys, various researchers have identified several advantages and disadvantages of the pulsed current technique [7-10]. In view of the problems involved in fusion welding of aluminum alloys, friction stir welding processes was used in the present study.

Friction stir welding process is based on frictional heat created by interface deformation, heat and solid-state diffusion [11]. FSW is a hot-working process in which a high amount of deformation is created by high speed rotating pin and shoulder and the temperature in the weld region rarely exceeds 0.8 times the melting temperature [Tm] in the work piece [12]. The process results in a variety of zones with different microstructures in precipitation hardenable aluminum alloys [13, 14&15]. The first attempt at classifying microstructures was made by Threadgill P.L [16]. This idea was further revised and accepted by the friction stir welding licenses association. Very few attempts were made to study the microstructure of dissimilar Al-alloy welds. No literature is available on the pitting corrosion behavior of dissimilar Al-alloy welds. The objective of present work is to study and compare the microstructural changes and pitting corrosion behavior when AA2014 and AA6061 alloy are welded in gas tungsten arc (fusion) welding and friction stir (solid state) welding processes.

2. Experimental Details

The parent metals used in this work are heat treatable wrought AA2014 and AA6061 alloys [thickness of plates is 4mm] in mill annealed (O) condition. The composition of the alloys and filler metal used in GTA welding is given in Table 1.Gas Tungsten Arc and Friction Stir welding processes were used in the present study. The parameters of the welding processes used are presented in Table 2 and 3.

Table 1 Chemical compositions of the base and filler materials used

Material	Cu	Mg	Si	Fe	Mn	Cr	Zn	Ti	Al
AA2014	4.5	0.4	0.8	0.7	0.8	0.1	0.25	0.15	Balance
AA6061	0.31	0.69	0.53	0.23	0.33	--	--	--	Balance
AA4043 (Filler)	0.25	0.05	5.20	0.80	0.05	--	--	--	Balance

Table 2 Input parameters used in continuous current GTA welding

Welding parameter	Current	Voltage	Welding speed	Shielding gas	Gas flow rate	Filler feed rate
Value	385A	7.2V	200mm/min	Argon	16 l/min	2200 mm/min

Table 3 Input parameters used in friction stir welding

Welding Parameter	Load	Speed of rotation	Speed of welding
Value	10.0 KN	800 rpm	135 mm/min

Before welding, the base material coupons and filler wire were thoroughly cleaned with brush and later with acetone. The welded samples were cut into convenient sizes and mounted in Bakelite for microstructural observation. After polishing with 120 to 600 grit SiC papers, the samples were

polished using alumina powder on rotating discs. Etching was done using Keller's reagent. The microstructures were recorded with Image analyzer attached to the Olympus made optical metallurgical microscope and also using scanning electron microscope (SEM). The pitting potentials of various regions of the welds were determined by using Potentio-dynamic polarization tests. Vickers hardness testing was carried out on weld/NZ, PMZ/TMAZ and HAZ+ regions of the samples with 5 kg load. Post weld heat treatment [Solution heat treated at 540^0C, 1 h + aged at room temperature for 30 days (T4)] was conducted on the welds and its effect on microstructure and pitting corrosion behavior was studied.

3. Results and discussion

3.1. Microstructure studies

3.1.1. Base Metal. In alluminium alloys the formation of intermetallic phases and precipitates basically depend mainly on the chemical composition of the alloy. The condition of the base alloy affects size and distribution of these phases. The Optical micrographs of the base metal AA2014 (in O and T4 conditions) are shown in Fig. 1. The microstructures reveal white matrix of α-solid solution grains and second phase particles appearing black in color. The optical microstructures of the aluminium alloy clearly show that relatively fine and uniformly distributed eutectics are present in T4 condition, where as coarse and non-uniformly distributed eutectics in O condition. SEM micrographs of base metal AA2014 in O and T4 conditions are shown in Fig. 2. Comparatively large particles (2-10μm) were present both within grains and at grain boundaries.

The EDX values of some randomly chosen particles indicated that Al/Cu weight ratio of these particles was close to that of about 53/47 for θ (Al_2Cu). The typical EDX spectrum of the particle is shown in Fig. 3. These particles will be considered as the θ phase as an approximation, even though they may contain very small amounts of other elements as well. Several small particles within the grains and along the grain boundaries (GBs) were believed to be θ phase, as they were too small to be analyzed by SEM-EDX.

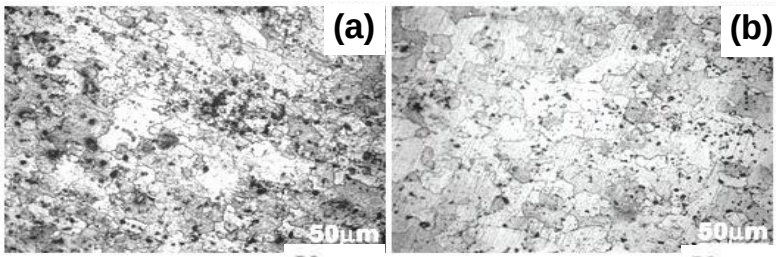

Fig. 1 Optical micrographs of base metal AA2014 (a) O condition (b) T4 condition

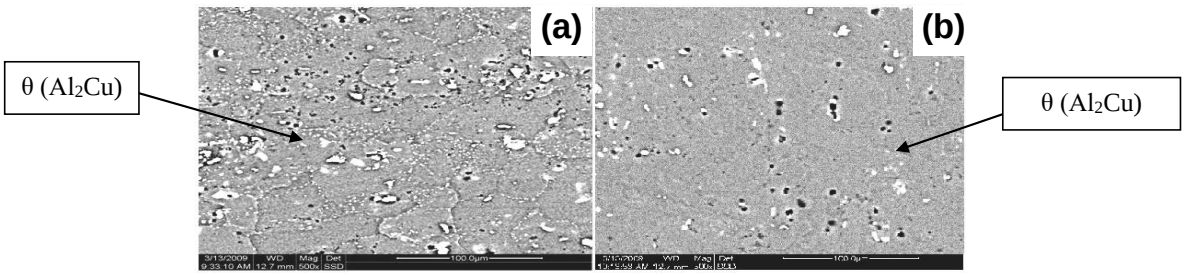

Fig. 2 SEM micrographs of base metal AA2014 (a) O condition (b) T4 condition

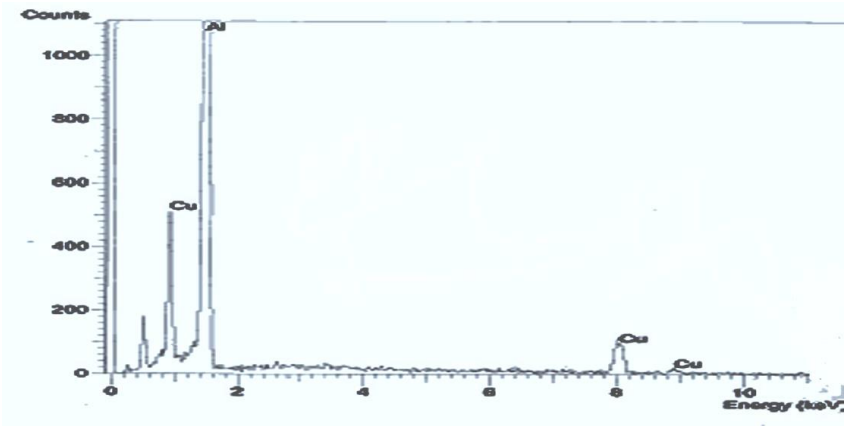

Fig. 3 EDX spectrum of AA2014-T4 particle

The solution heat-treating temperature for AA2014 alloy is 540^0C. From the phase diagram (Fig. 4) the base metal is expected to consist of α-matrix plus additional undissolved θ ($CuAl_2$) particles [17].

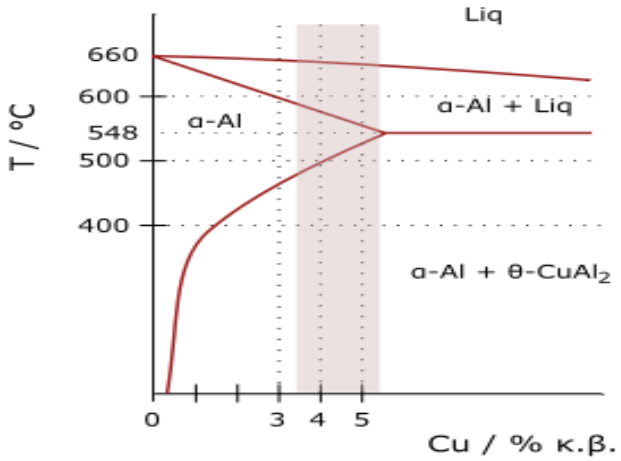

Fig. 4 Al-Cu phase diagram

3.1.2. Gas Tungsten Arc Welds

Formation of fusion and partially melted zones in dissimilar AA2014-AA6061 GTA welds in O condition is shown in Fig. 5. It consists of five zones. 1) Fusion Zone (FZ) where the intermixing of AA2014 and AA6061 alloys has taken place 2) PMZ on AA2014 side 3) PMZ on AA6061 side 4) HAZ on AA2014 side and 5) HAZ on AA6061 side. Cast structure is clearly visible in FZ, where as in PMZ coarsening of eutectics was observed.

Optical micrograph of the fusion zone of dissimilar AA2014-AA6061 GTA weld is shown in Fig. 6. The microstructure of fusion zone in O condition (Fig. 6a) revealed the eutectics of $CuAl_2$ and Mg_2Si appearing in the dendritic matrix of α-solid solution. The eutectic was formed as thick and continuous network in the fusion zone. The optical micrograph of fusion zone of dissimilar GTA weld in PWHT condition (Fig. 6b) clearly indicated that the grain coarsening occurred after PWHT due to the solution treatment and ageing involved in the process.

The formation of the PMZ in dissimilar AA2014-AA6061 GTA welds is clearly understood from Fig. 5. It is evident from the micrographs that the thickness of the PMZ is relatively more on AA2014 side than that of AA6061 side. This is attributed to more heat transferred on AA2014 side because of the high thermal conductivity of the copper present in the alloy.

Whereas on AA6061 side the PMZ is very narrow which indicated its relatively low thermal conductivity.

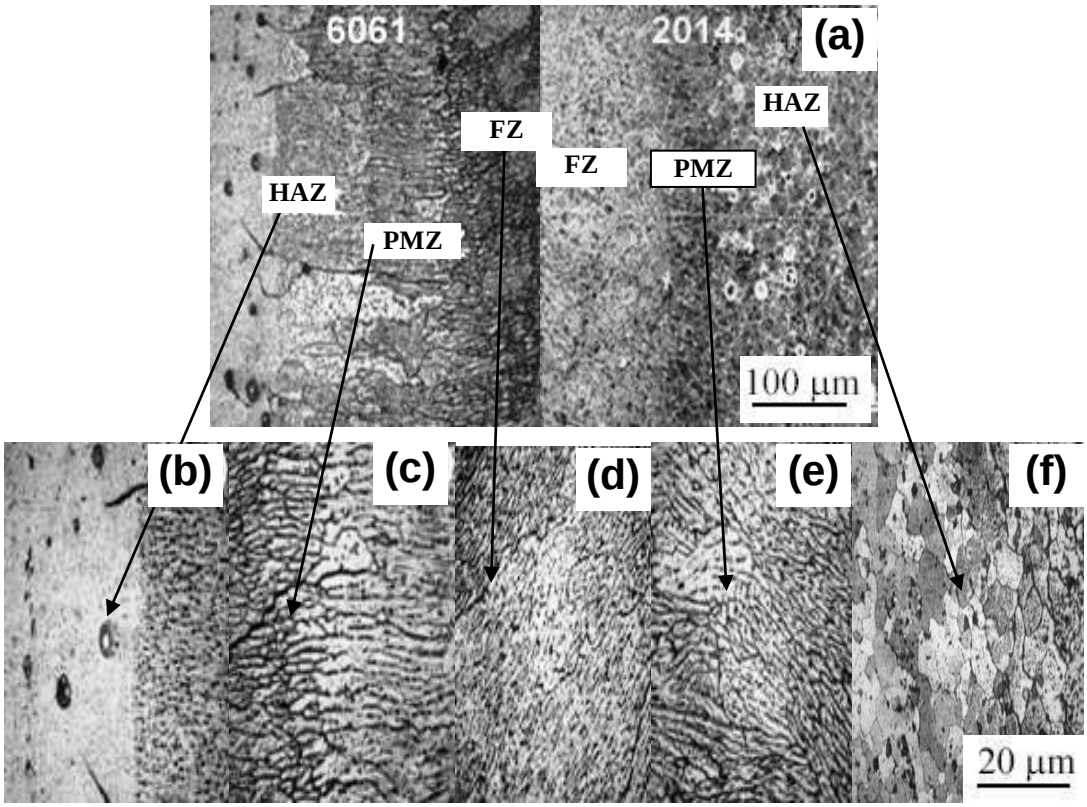

Fig. 5 Optical microstructures ofAA2014-AA6061GTA welds in O condition (a) Formation of PMZ (b) HAZ [AA6061] (c) PMZ [AA6061] (d) FZ(e) PMZ [AA2014] (f) HAZ [AA2014]

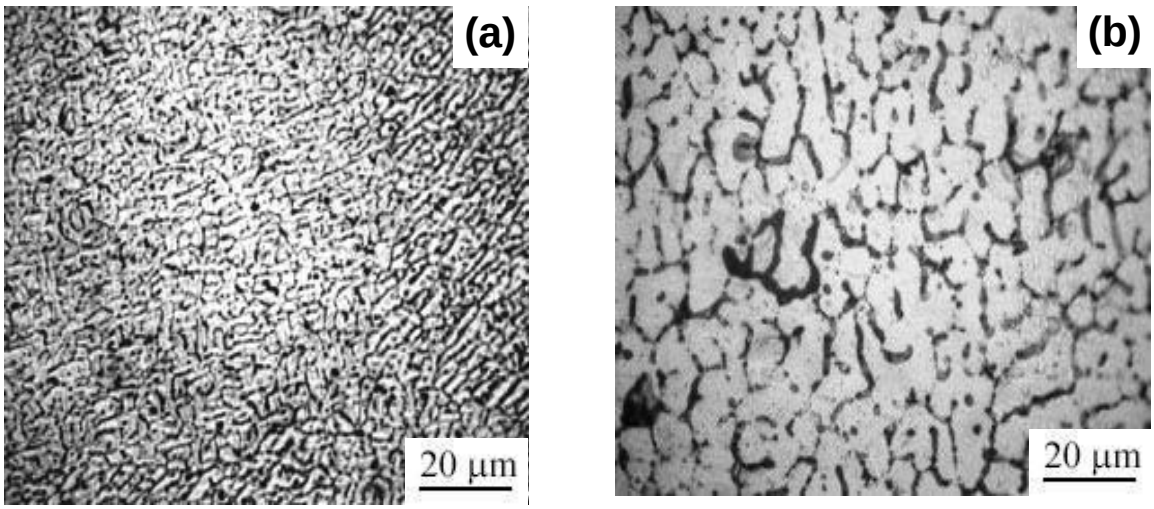

Fig. 6 Optical micrographs of FZ in AA2014-AA6061 GTA welds a) O condition b) PWHT condition

Optical and SEM micrographs of partially melted zone of dissimilar GTA welds in O condition shown in Fig. 7 clearly revealed darkly etched grain boundaries indicating liquation in the PMZ. The grain boundary filled with eutectic liquid was also seen in optical and SEM

micrographs. In general, aluminum liquid that is richer in Si is considered to be more fluid. Therefore penetration should be easier for the AA4043 filler and the lower solidus temperature of the AA4043 might have promoted liquid penetration into the PMZ for a longer distance. The possible eutectic reactions causing liquation in PMZ of the welds of AA6061 are as follows [18]:

i) $\alpha + Si \longrightarrow L$ at 577^0C

ii) $\alpha + Mg_2Si + Si \longrightarrow L$ at 555^0C

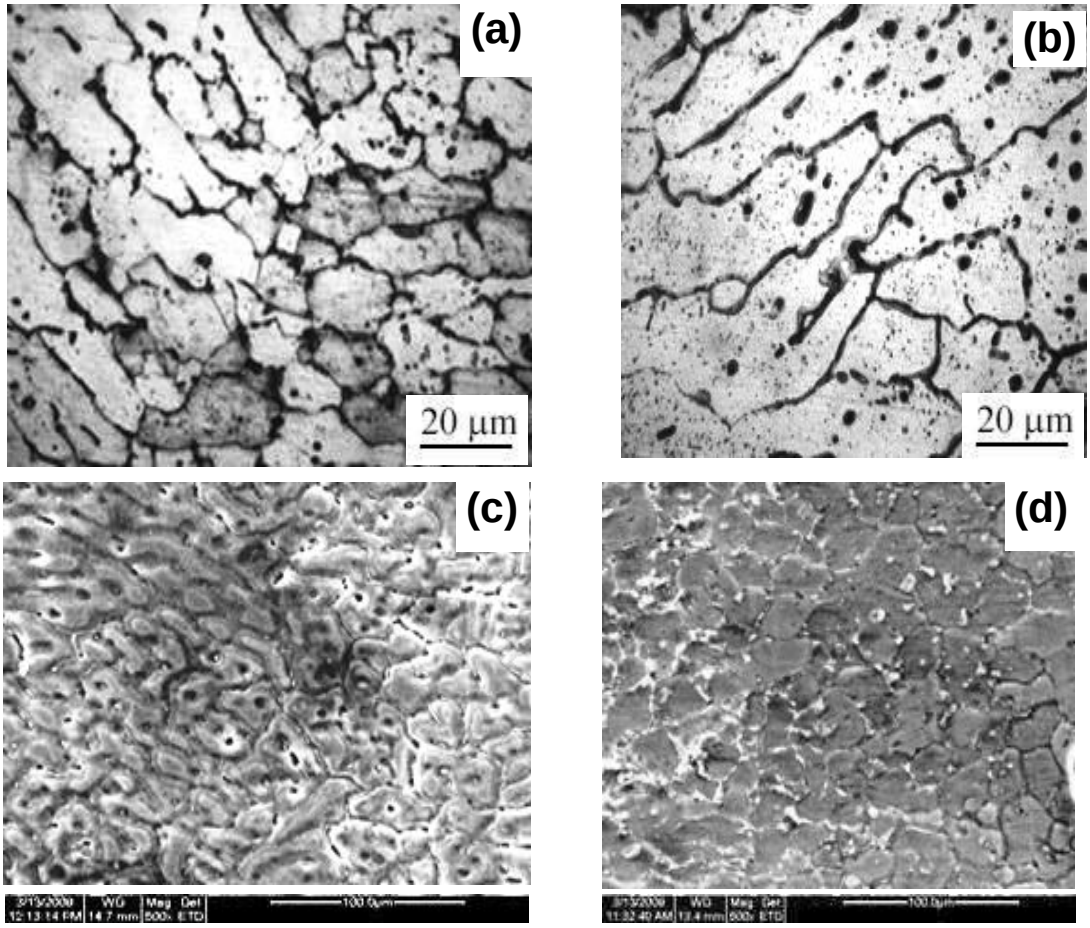

Fig. 7 Optical and SEM micrographs of PMZ in AA2014-AA6061 GTA welds in O condition(a) Optical of AA2014 side (b) Optical of AA6061 side (c) SEM of AA2014 side (d) SEM of AA6061 side

SEM-EDX values were taken at two different locations of PMZ i.e. one at grain boundary (P1) and the other at matrix (P2) and the values in O condition are given in Table 4. From the EDX values it was noticed that the silicon diffused towards AA2014 side (13.95% Si against 0.8% present in the base metal). This may be due to dilution of silicon at temperatures between liquidus and solidus temperatures.

Fig. 8 shows the optical microstructures of PMZ on AA2014 and AA6061 sides of GTA weld in PWHT condition. From the microstructures it is evident that the eutectics are relatively fine and continuous in PMZ on AA2014 side whereas on AA6061 side these are relatively coarse and discontinuous. This is attributed to the dissolution of eutectics in the solid solution in solution treatment and subsequent re-precipitation during ageing of PWHT.

Table 4 Composition (in Wt.%) of particles in PMZ (SEM-EDX) ofAA2014-AA6061 GTA welds in O condition

(a) AA2014 side

Position	Mg	Al	Si	Cu
P1 (GB)	03.65	76.44	13.95	14.70
P2 (Matrix)	03.01	90.77	03.46	01.19

(b) AA6061 side

Position	Mg	Al	Si	Cu
P1 (GB)	01.42	59.52	10.93	02.19
P2 (Matrix)	02.08	93.05	01.81	01.84

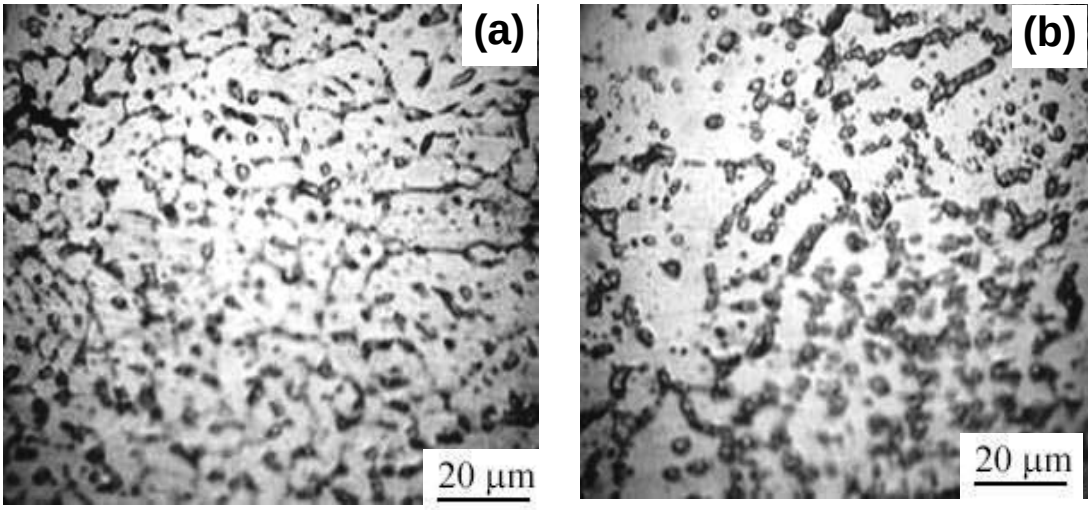

Fig. 8 Optical micrographs of PMZ in AA2014-AA6061 GTA welds in PWHT condition (a) AA2014 side (b) AA6061 side

*3.1.3. Friction stir welds.*The formation of nugget zone (NZ) and TMAZ in dissimilar AA2014-AA6061 friction stir weld in O condition is shown in Fig. 9. During FSW of dissimilar materials mechanical mixing of the materials occurs. Lamellar like shear bands are well noticed on the top of the NZ. The Nugget Zone is the region that experienced the highest strain and undergoes recrystallization as shown in Fig. 10. Its microstructure is due to mechanical action of the tool probe that generates a continuous dynamic recrystallization process. The higher temperature and the severe plastic deformation during the welding in the stirred zone resulted in a new equiaxed fine grain structure [19] both for AA2014 and AA6061.

The quantitative SEM-EDX is performed on a line at points in the nugget zone (NZ) to see any diffusion has taken place at the interface and is shown in Fig. 11. The concentration profile of dissimilar friction stir weld in PWHT condition as shown in Fig. 12 revealed that no diffusion has taken place at the interface. This suggests that just away from the weld centerline on either side, the respective base materials predominantly govern and constitute the NZ. It is well known that there must be sufficient time and temperature for diffusion of alloying elements for making homogeneous welds in terms of chemical composition. Even though the NZ experiences a temperature sufficiently high enough to promote diffusion, the welding time is too short to achieve homogenization by diffusion and hence inherent differences in chemistry resulted in the stir zone. The above observation is in line with a work on dissimilar FSW between AA 6056 and AA 7075 by Bala Srinivasan et al. [20] and by Shigematsu et al. [21] between AA 5083 and AA6061.

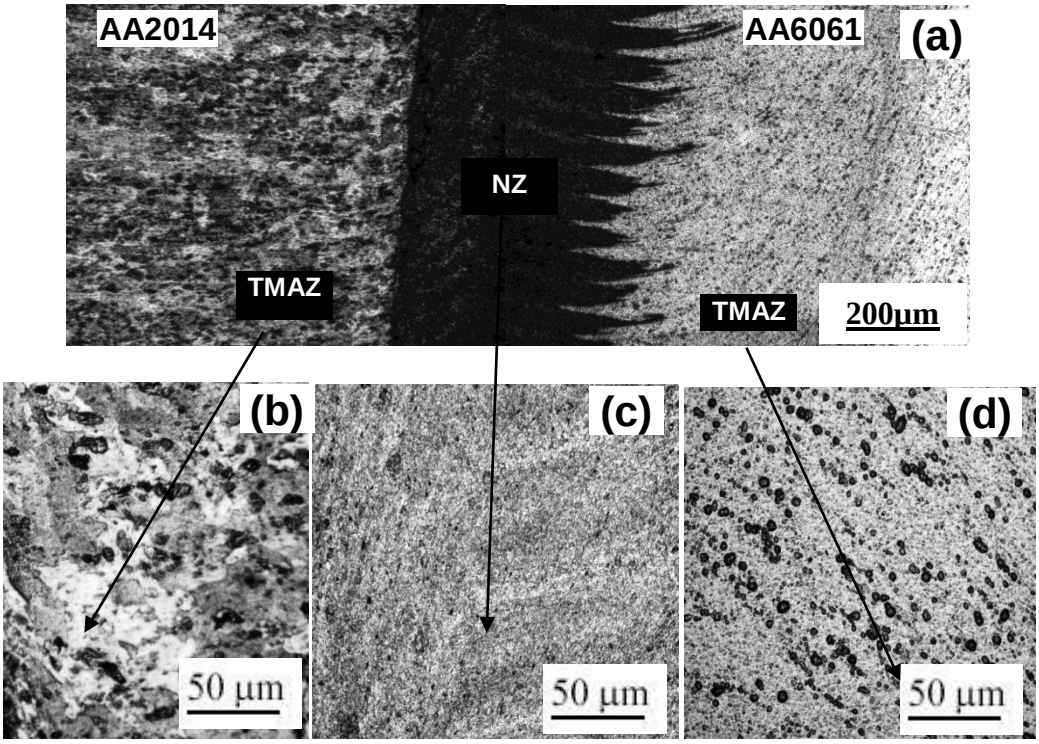

Fig. 9 Optical microstructures of AA2014-AA6061 friction stir welds in O condition
(a) Formation of nugget zone (b) TMAZ (AA2014)(c) NZ (d) TMAZ (AA6061)

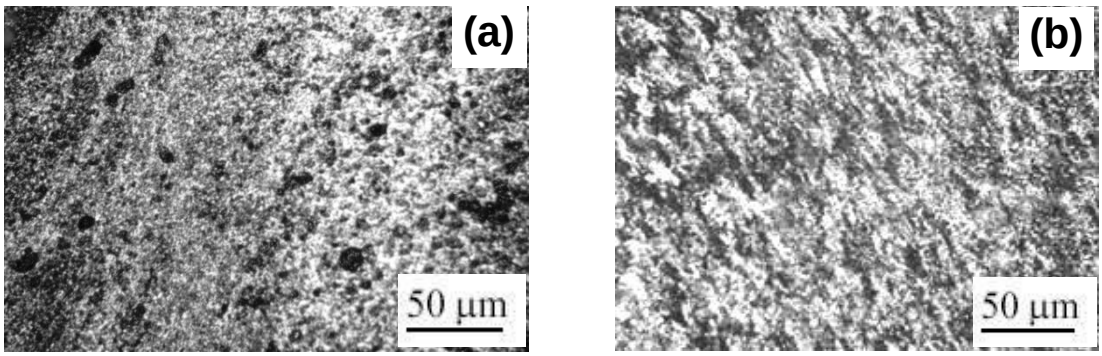

Fig. 10 Optical micrographs of NZ inAA2014-AA6061friction stir welds (a) O condition (b) PWHT condition

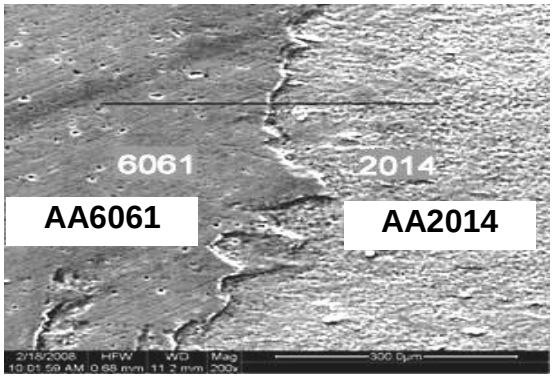

Fig. 11SEM micrograph of the NZ interface in AA2014-AA6061 friction stir welds in PWHT condition

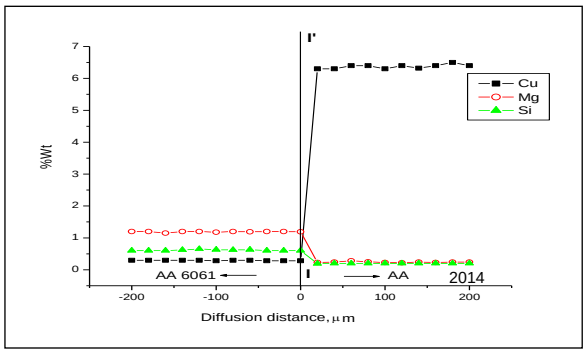

Fig. 12 Concentration profile of the NZ interface in AA2014-AA6061 friction stir weld in PWHT condition

On both sides of the nugget zone thermo-mechanically affected zones (TMAZs) are observed which contain highly deformed grains resulted from the stirring action and where no recrystallization was observed (Fig. 13). It may be attributed to the fact that the temperature, derived from the process, was not high enough and deformation was not so adequate to cause recrystallization.

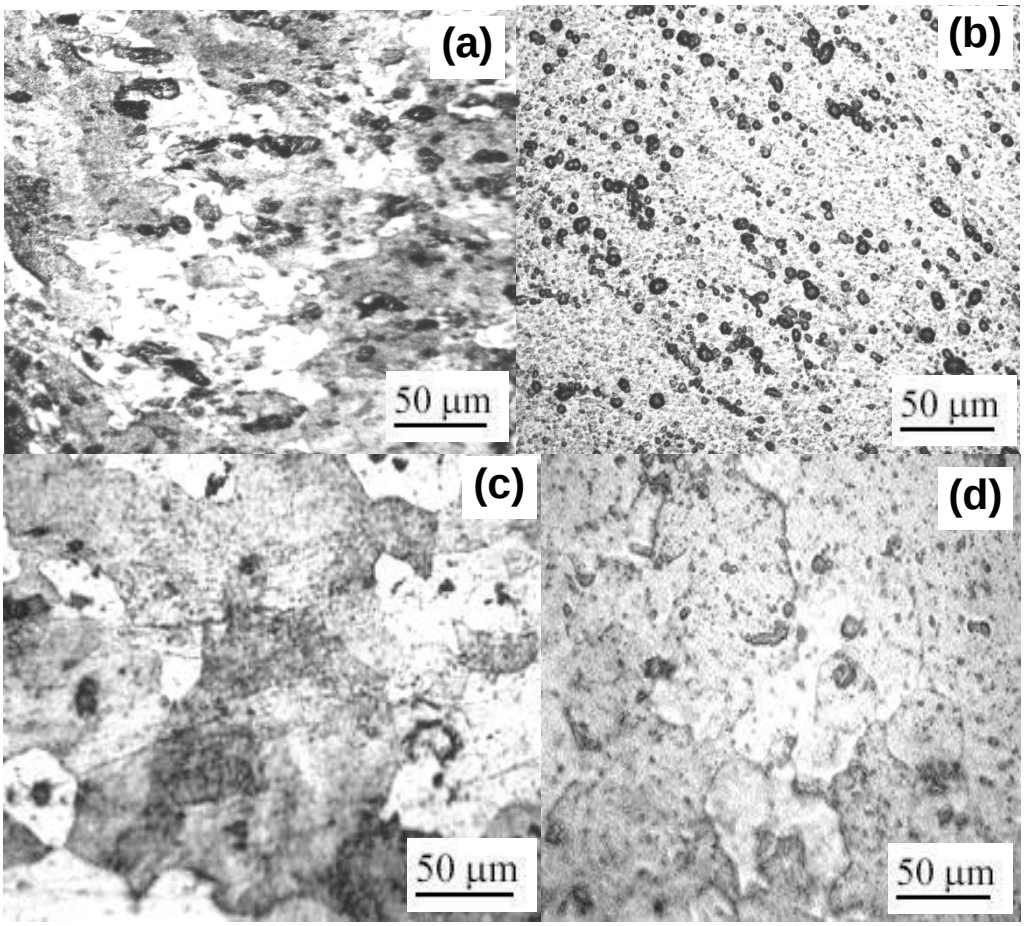

Fig. 13 Optical micrographs of TMAZ in AA2014-AA6061friction stir welds(a) AA2014 side of O condition (b) AA6061 side of O condition(c) AA2014 side of PWHT condition (d) AA6061 side of PWHT condition

3.2. Hardness studies

The hardness values of the dissimilar GTA weld in O and PWHT conditions are given in Table 5. It is observed that the hardness of FZ is increased after PWHT. This is attributed to modification of cast structure into naturally aged structure where coherency between matrix and precipitates is the main reason for the increase in hardness.

Table 5 Vickers hardness values of AA2014-AA6061 GTA welds

Condition	PMZ AA2014	FZ	PMZ AA6061
O	115-125	74-78	70-78
PWHT	98-105	92-96	80-86

Vickers hardness values of dissimilar AA2014-AA6061 friction stir welds in O and PWHT conditions are given in Table 6. Increased hardness values are observed in the weld after PWHT. This is attributed to the possible formation of coherent precipitates likeθ' in AA2014 and β' in AA6061 alloy. Precipitation of eutectics in all zones of the weldment was observed which may be the reason for the increased hardness throughout the weld cross section after PWHT.

Table 6 Vickers hardness values of AA2014-AA6061 friction stir welds in O and PWHT conditions

Condition	TMAZ (AA2014)	NZ	TMAZ (AA6061)
O	62-65	76	50-55
PWHT	75-81	85	66-70

From the above tables 5 and 6, it is observed that when compared to GTA welds the hardness values in FS welds are lower in all regions. It is attributed to the fact that the GTA welds have cast structure in fusion zone (FZ) and FSW welds have nugget zone (NZ) which is of mechanically mixed elements. The PMZ in GTA welds will be generally harder than nugget zone in FS welds where the effect of heat on microstructure is very less.

3.3. Pitting corrosion studies

Table 7 gives the E_{pit} values of dissimilar AA2014-AA6061 GTA welds in O and PWHT conditions. It is interesting to observe here that the pitting corrosion resistance of the dissimilar welds in all regions was improved by post weld heat treatment. This is because of precipitation of very fine submicroscopic particles from supersaturated solution during natural ageing.

Table 7 Pitting potentials, E_{pit}(mV), SCE of AA2014-AA6061 GTA welds in O and PWHT conditions

Condition	PMZ/HAZ (AA2014)	FZ	PMZ/HAZ (AA6061)
O	-676	-634	-662
PWHT	-645	-618	-632

Potentio-dynamic polarization curves of PMZ of dissimilar GTA welds in O and PWHT conditions as shown in Fig. 14(a) also confirmed that the PWHT of the dissimilar welds improved the corrosion resistance.The E_{pit} values of friction stir welds are given in Table 8. From the table it is evident that the pitting corrosion resistance of the welds after PWHT is improved in all regions of the weld.Potentio-dynamic polarization curves of TMAZ/HAZ of dissimilar AA2014-AA6061 friction stir welds on AA6061 side in O and PWHT conditions are shown in Fig. 14(b). These curves also revealed the similar trend i.e. PWHT improved the pitting corrosion resistance of the TMAZ/HAZ. Low pit density was observed in PWHT condition in friction stir welds. This is in agreement with the pit potential data of the welds (Fig. 15(d)).

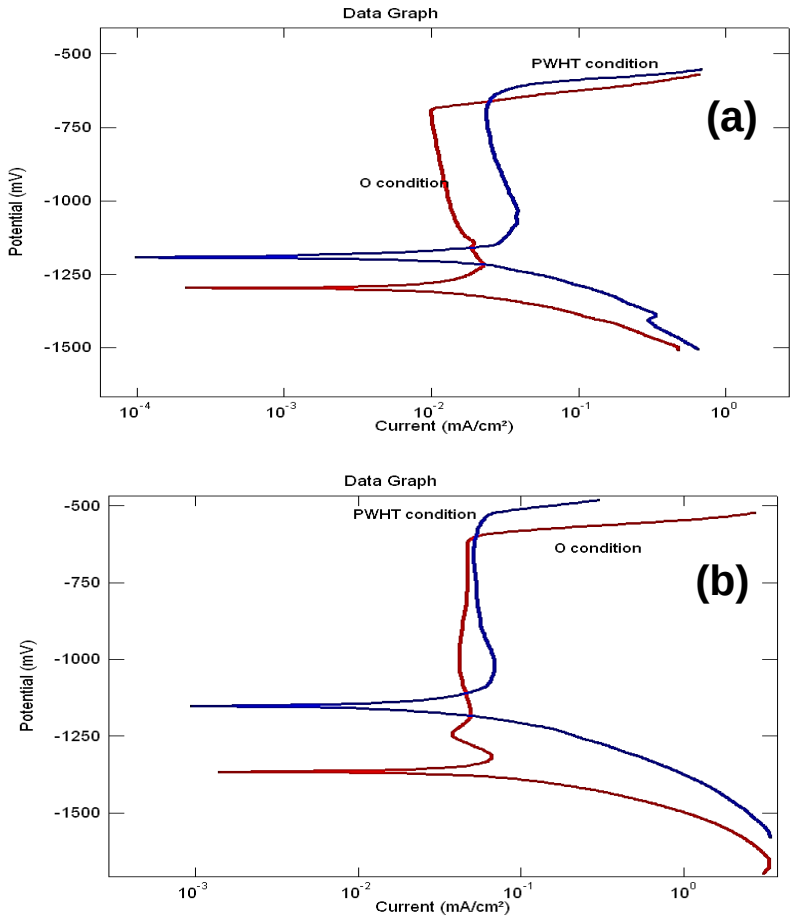

Fig. 14 Potentio-dynamic polarization curves of (a) PMZ on AA6061 side in AA2014-AA6061GTA welds in O and PWHT condition (b) TMAZ/HAZ on AA6061 side ofAA2014-AA6061friction stir welds in O and PWHT conditions

Fig. 15 shows the optical micrographs of dynamic polarized PMZ on AA6061 side of AA2014 - AA6061 GTA welds in O condition and PWHT condition and TMAZ/HAZ on AA6061 side of AA2014-AA6061 friction stir welds in O condition and in PWHT condition after corrosion test. From the microstructures it is evident that the pit density is more in O condition than that of PWHT condition. The pit density confirmed that the PWHT improved the pitting corrosion resistance of the weld joint. The pitting potential values of GTA and FS welds are compared in Table 9. It is observed that the pitting corrosion resistance of the FS welds in all regions is better than GTA welds. This is attributed to the fact that cast structure in GTA welds generally will have less corrosion resistance when compared to the nugget zone of FS welds.

Table 8 Pitting potentials, E_{pit}(mV), SCE of AA2014-AA6061 friction stir welds in O and PWHT conditions

Condition	TMAZ/HAZ (AA2014)	NZ	TMAZ/HAZ (AA6061)
O	-660	-607	-625
PWHT	-535	-525	-531

Table 9 Pitting potentials, E_{pit} (mV), SCE ofAA2014-AA6061GTA and FS welds in PWHT condition

Weld	PMZ /TMAZ and HAZ (AA2014)	FZ/NZ	PMZ /TMAZ and HAZ (AA6061)
GTAW	-645	-618	-632
FSW	-535	-525	-531

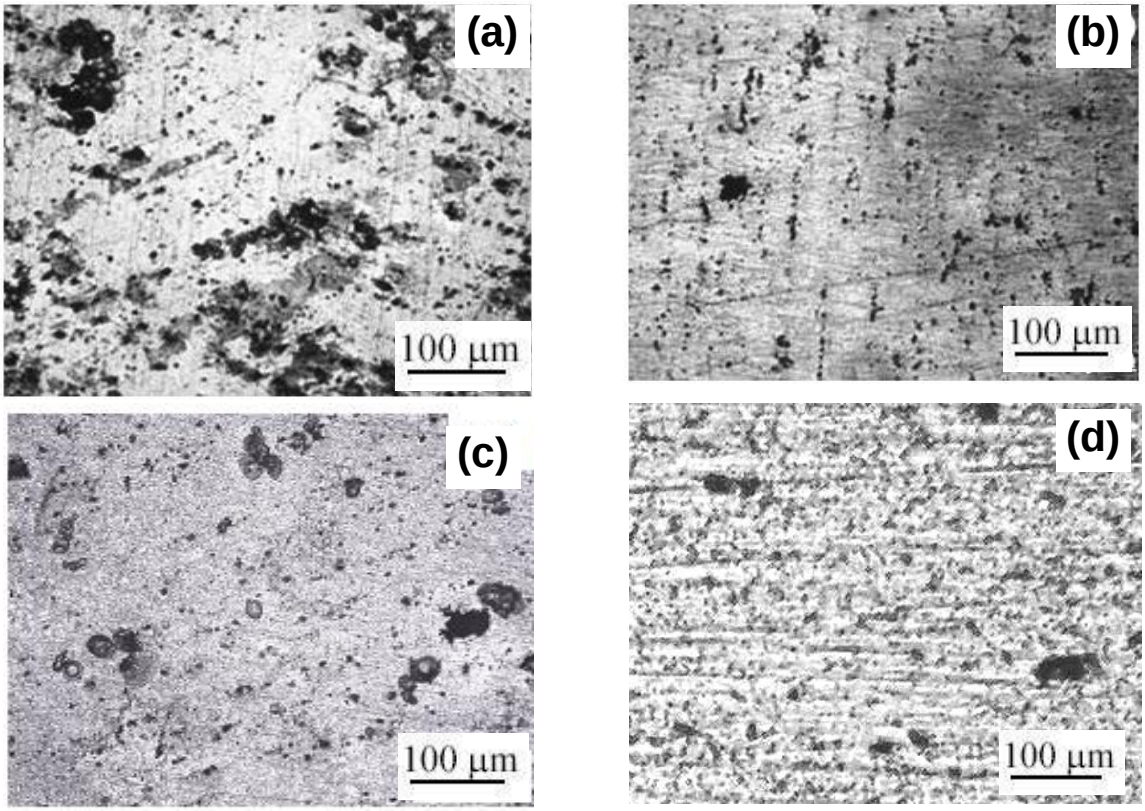

Fig. 15Optical micrographs of dynamic polarized (a) PMZ on AA6061 side of AA2014 -AA6061GTA welds in O condition (b) PMZ on AA6061 side of AA2014 -AA6061 GTA welds inPWHT condition (c) TMAZ/HAZ on AA6061 side of AA2014-AA6061 friction stir welds in O condition (d) TMAZ/HAZ on AA6061 side of AA2014-AA6061 friction stir welds in PWHT condition

4. Conclusions

1. Microstructures of the two base metals chosen in this work (AA2014 and AA6061) clearly revealed the differences in the distribution of eutectics. Relatively fine and uniformly distributed eutectics are present in T4 condition, whereas coarse and non-uniformly distributed eutectics are present in annealed condition.
2. In GTA welds of AA2014-AA6061 alloys in annealed condition, Cast structure is clearly visible in fusion zone whereas coarsening of eutectics was observed in partially melted zone.
3. Fusion zone of dissimilar GTA weld in PWHT condition clearly indicated that the grain coarsening occurred after PWHT due to the solution treatment and ageing involved in the process. It is evident that the thickness of the PMZ is relatively more on AA2014 side than that of AA6061 side.
4. In FS welds, Lamellar like shear bands are well noticed on the top of the stir zone. The concentration profile of dissimilar friction stir weld in T4 condition revealed that no diffusion has taken place at the interface.

5. Poor Hardness is observed in all regions of FS welds compared to that of GTA welds is due to grain coarsening and dissolution of strengthening intermetallic precipitates.
6. The pitting corrosion resistance of the dissimilar FS welds in all regions was improved by post weld heat treatment. This is attributed to precipitation of very fine submicroscopic particles from supersaturated solution during natural ageing and dissolution of secondary intermetallic precipitation helps in reduction of active sites for pit initiation.

References

[1] Liptak, J.A. and Baysinger, F.R. "Welding Dissimilar Aluminum Alloys", *Welding Journal*, pp. 173s-180s, 1968.
[2] Luijendijk T. Welding of dissimilar aluminum alloys. *J Mater Process Technol* ,pp 2000;103 ;29-35.
[3] Huang. C and S. Kou., Partially melted zone in aluminium welds-liquation mechanism and directional solidification, *Welding Journal*, 2000, 79; 113s-120s.
[4] Huang. C and S. Kou., Liquation mechanisms in multi component aluminium alloys during welding, *Welding Journal*, 2002, 81, 211s-222s.
[5] Huang. C and S. Kou., Partially melted zone in aluminium welds-planar and cellular solidification, *Welding Journal*, 2001, 80, 46s-53s.
[6] Huang. C and S. Kou., Partially melted zone in aluminium welds-solute segregation and mechanical behaviour, *Welding Journal*, 2001, 80, 9s-17s.
[7] Garland J.G., weld pool solidification control. British Welding journal, 1974, 22, 121-127.
[8] Reddy G.M., Weld microstructure refinement in a 1441 grade Al-li alloy, *J.Mater.Sci.*, 1997, 32, 4117-4126.
[9] Yamamoto, H., S. Harada, T. Ueyama, S. Ogawa, F. Matsuda and K. Nakata., Beneficial effects of low frequency pulsed MIG welding on grain refinement of weld metal and improvement of solidification cracking susceptibility of aluminium alloys,*Welding International*,1993, 7 (6), 456-461.
[10] Janaki Ram, G.D., G.M. Reddy and S. Sundaresan., Effect of pulsed welding current on the solidification structures in Al-Li-Cu and Al-Zn-Mg alloy welds, *Practical Metallography*, 2000, 37 (5), 276-288.
[11]. Rhodes C G, Mahoney M W, Bingel W H, Spurling R A and Bampton C C, *ScriptaMaterialia*, 36, (1997) 69
[12]. Dawes C J and Thomas W M, *Welding Journal*, 75(1996) 41.
[13]. Flores, Olga V K, Christine M L E, Brown D P,Brook M, and McClure J.C., *ScriptaMaterialia*, 38,(1998) 703.
[14]. Murr L E, Li Y, Elizabeth A, Flores R D andMcClure J C., *Jrnl. Of materials processing and manufacturing science*, 7, (1998) 145.
[15]. Liu G, Murr L E, Niou C S, McClure J C, VegaF R, *Scripta Materialia*, 37, (1997) 355.
[16] Threadgill P.L (1999) Friction stir welding – the state of art, Bulletin 678; The welding Institute; Abington, Cambs; UK
[17] Polmear I.J (1997) Wrought aluminium alloys. *Materials Science forum*, 21; 1-26.
[18] Mondolfo L.F (1976) Aluminium alloys: Structure and properties. Butterworths & Co Ltd, Masachusetts, 717-857
[19] Hassan Kh.A.A, A.F. Norman, D.A. Price, P.B. Prangnell (2003) Stability of nugget zone grain structures in high strength Al-alloy friction stir welds during solution treatment. *Acta Materialia*, 51; 1923–1936.
[20] Bala Srinivasan P, W. Dietzel, R. Zettler, J.F. dos Santos, V. Sivan (2005) Stress corrosion cracking susceptibility of friction stir welded AA7075–AA6056 dissimilar joint. *Materials Science and Engineering*, A 392; 292–300
[21] Shigematsu I, Y.J. Kwon, K. Suzuki, T. Imai, N. Saito (2003) Joining of 5083 and 6061 aluminum alloys by friction stir welding. *J. Mater. Sci. Lett.*, 22; 343–356.